Work Hardening of Austenitic Manganese Hardfacing Deposits

Hardness and tensile tests are not discriminatory, but a dropweight indentation test discriminates among various alloy types

BY D. J. KOTECKI AND V. B. RAJAN

ABSTRACT. Four test methods were investigated for their ability to discriminate among various austenitic manganese hardfacing deposits as regards work hardening capacity. The test methods are 1) Rockwell C testing in Brinell hardness impressions made with varying loads, 2) Meyer's Law applied to Brinell impressions made with varying loads, 3) tensile testing and 4) a newly devised dropweight indentation test. Of these, only the dropweight indentation test discriminated successfully among ordinary 14% Mn austenitic manganese steel, rich 20% Mn austenitic manganese steel and 15% Mn–15% Cr austenitic manganese steel. The two more highly alloyed austenitic manganese compositions were found to offer higher resistance to indentation than do the ordinary austenitic manganese compositions. These results are being applied to high impact situations such as rail frogs.

Introduction

Austenitic manganese steel, also known as Hadfield manganese steel, is hardly a new engineering material, having been patented in 1884 (Ref. 1). Steels of this type are well known for their work hardening ability. More than 40 years passed after the first patent, however, before this steel was applied in the form of a hardfacing deposit from arc welding electrodes (Refs. 2, 3). Today, their use is widespread, with service in rock crushing, automobile shredding, railroad frogs and switches and numerous other applications requiring resistance to heavy impact or gouging.

Austenitic manganese steel hardfacing deposits are commonly selected for their ability to work harden rapidly, providing resistance to impact wear. Over the years, common commercial practice has evolved into minor variations within three more or less standardized typical all-weld-metal deposit composition families. These are 1) a basic composition range, similar to the base metal composition range, nominally about 0.7–1.0% C, 14% Mn, sometimes with a few percent of Ni and/or Cr, which is referred to herein as "ordinary austenitic manganese" and coded "M14"; 2) an enriched composition range, nominally about 0.9–1.1% C, 20% Mn or more, 5% Cr, which is referred to herein as "rich austenitic manganese" and coded "M20"; 3) and a composition range in which the chromium approximately equals the manganese, nominally about 0.3–0.5% C, 15% Mn, 15% Cr, which is referred to herein as "austenitic manganese-chrome" and coded "MC15."

Claims are made that one composition or another work hardens more rapidly, therefore making it a better choice for rebuilding, for example, rail frogs, where minimal mushrooming is desirable. Such claims are seldom, if ever, substantiated by experimental evidence. The present work was undertaken to evaluate various laboratory tests related to measuring work hardening of these three families of austenitic manganese steel hardfacing deposits. The objective is to find a test that discriminates among these families in a quantitative fashion.

D. J. KOTECKI and V. B. RAJAN are with The Lincoln Electric Company, Cleveland, Ohio.

KEY WORDS

Dropweight
Indentation Test
Hardfacing Deposits
Manganese
Meyer's Law
Rockwell C Testing
Railroad Frogs
Tensile Testing

Experimental Procedure

Electrodes

Eight commercially available self-shielded flux cored arc welding (FCAW) wires, $\frac{7}{64}$ in. (2.8 mm) diameter, were obtained, representing three filler metal manufacturers and all three austenitic manganese alloy families. A multipass buildup, more than $1\frac{1}{2}$ in. (38 mm) thick, approximately 16 in. (400 mm) long and approximately 5 in. (125 mm) wide, was produced with each wire on 1-in. (25-mm) thick mild steel base metal. The welding conditions used in this work are given in Table 1 and are within the range of welding conditions recommended by the manufacturer of each electrode. From each buildup, an all-weld-metal tensile specimen of $\frac{1}{2}$-in. (12.7-mm) reduced section diameter and 2-in. (51-mm) gauge length was machined and tested following standard procedures given in ANSI/AWS B4.0. Chips for chemical analysis were machined from the top layer of each buildup. These were analyzed for carbon, sulfur and nitrogen by fusion methods and for chromium, manganese, nickel, silicon, molybdenum and vanadium by wet chemical methods.

Test Specimens

A cross section of each buildup, approximately $\frac{3}{8}$ in. (10 mm) thick, was cut and ground for hardness determinations. In addition to both normal Brinell (10-mm-diameter tungsten carbide ball indenter) and Rockwell C hardness measurements, Rockwell C measurements were made in the center of Brinell dents

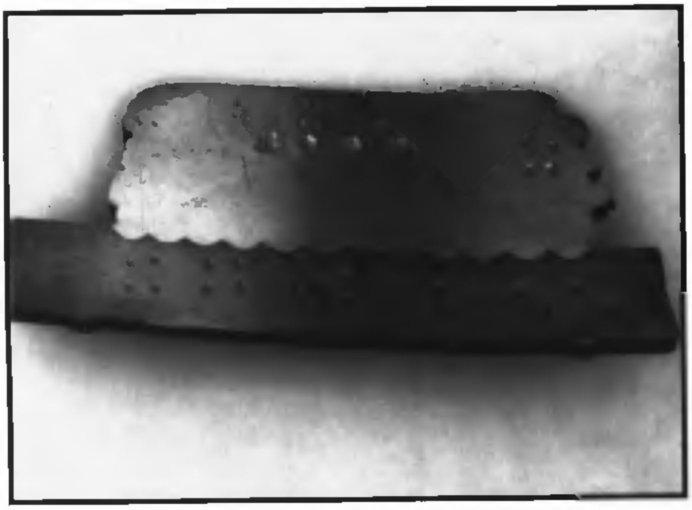

Fig. 1 — Cross section of an austenitic manganese hardfacing deposit.

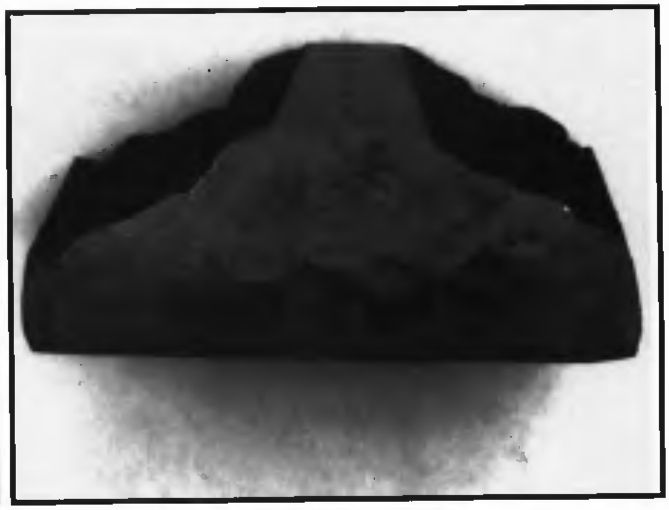

Fig. 2 — Segment of pyramidal deposit of austenitic manganese used for machining dropweight test specimen (see Figs. 3 and 4).

Table 1 — FCAW Welding Conditions for Austenitic Manganese Hardfacing Deposits

A36 Base Metal	18 by 5 by 1 in. (460 by 127 by 25 mm)
Wire Diameter	7/64 in. (2.8 mm)
Wire-Feed Speed	150 in./min (3.8 m/min)
Contact Tube to Work Distance	1¾ in. (44 mm)
Wire Feeder to Work Voltage	29 Volts, DCEP
Shielding Gas	None
Travel Speed	15 in./min (380 mm/min)
Interpass Temperature, maximum	300°F (150°C)
Buildup Height	1½ in. (38 mm)

Table 2 — All-Weld-Metal Deposit Compositions for FCAW Wires

FCAW	Deposit Composition, %							
Wire	C	Mn	Si	Cr	Ni	Mo	V	N
M14A	0.97	14.25	0.42	3.51	2.73	0.01	0.008	0.065
M14B	0.58	13.25	0.45	5.19	0.57	0.01	0.042	0.103
M14C	1.03	15.00	0.38	3.51	0.37	0.01	0.012	0.072
M20A	1.01	20.0	0.24	5.15	0.04	0.01	0.010	0.050
M20B	1.07	25.5	0.17	4.59	0.00	0.00	0.000	0.091
MC15A	0.40	16.5	0.25	13.5	0.07	0.01	0.026	0.213
MC15B	0.41	15.0	0.43	17.8	0.03	0.01	0.012	0.096
MC15C	0.28	15.5	0.23	18.4	0.89	0.01	0.022	0.295

that had been made under various loads — 500, 1000, 1500, 2000, 2500 and 3000 kg. This allowed Rockwell C measurement after varying, controlled, degrees of deformation.

Note that a Rockwell C hardness reading in the center of a 3000-kg Brinell dent is a fairly standard, if informal, test used by several filler metal manufacturers for developing work hardening results. There is no standard for this approach. It is recognized that the bottom of the Brinell dent is not quite flat (as required for a correct Rockwell C measurement), and that the Rockwell C impression is often not quite centered in the Brinell dent. Nevertheless, qualitative comparisons of work hardening are often made in this fashion.

In addition, clusters of overlapping 3000-kg Brinell dents were made in each sample to produce still more work hardening, and a Rockwell C impression was made in the center of the last overlapping dent. Figure 1 shows a cross section of one of the buildups after all of the hardness impressions were made. As another means of looking at work hardening, parallel flat surfaces about ¼ in. (6 mm) wide were ground on the reduced section of each broken tensile test specimen. The broken tensile specimen was then given Rockwell C impressions, 3000-kg Brinell dents, and then a Rockwell C impression was made in the center of each Brinell dent. All hardness values reported for this work are averages of at least four individual readings.

When all of the above tests failed to find clear discrimination among the austenitic manganese hardfacing deposits, a dropweight test was conceived. Niconoff (Ref. 4) used repeated dropweight testing to examine the strain hardening distribution below the surface after repeated impacts on austenitic manganese base metals, varying the dropweight energy from 12.5 to 200 ft-lb (17 to 271 J). Niconoff's test sample was a cone with a 60-deg included angle point; the hammer (a flat surface) was dropped on the original point of the cone.

Since the alloys under study in the present program are directed at rail frogs, where resistance to indentation, not distribution of strain hardening below the surface, is the key feature, a modification of Niconoff's approach was adopted. For each composition under test, a pyramidal buildup was made on ½-in. (12.7-mm) thick mild steel bar stock 3 in. (76 mm) wide. The first layer of buildup consisted of six passes, the second of five passes, and so on until the sixth layer consisted of one pass. Figure 2 shows a segment sectioned out of one of the pyramidal deposits. By trial and error, a convenient test specimen size was found that could be machined from the pyramidal buildup. Dimensions were held to tight tolerances so that the initial area of impact and the initial height of buildup would be consistent from one sample to the next. Figure 3 shows the specimen dimensions finally adopted. In all cases, the base of the machined specimen consisted partly of mild steel base metal and

Table 3 — Tensile and Hardness Test Results

Deposit Type		Ordinary austenitic manganese			Rich austenitic manganese		Austenitic manganese-chrome		
Test Specimen	A36	M14A	M14B	M14C	M20A	M20B	MC15A	MC15B	MC15C
Tensile, ksi (MPa)	N.M.	101.2 (698)	118.3 (816)	117.8 (812)	126.3 (871)	129.0 (889)	128.8 (888)	137.9 (951)	120.8 (833)
Yield, ksi (MPa)	N.M.	86.6 (597)	79.0 (545)	89.5 (617)	92.0 (634)	101.0 (696)	87.9 (606)	93.5 (645)	101.9 (703)
% Elongation	N.M.	11	19	16	23	24	33	31	10
500 kg Brinell	136	186	197	164	202	192	205	205	219
1000 kg Brinell	155	220	237	229	257	236	244	225	244
1500 kg Brinell	163	235	246	242	276	250	261	240	255
2000 kg Brinell	165	238	257	250	282	259	253	248	275
2500 kg Brinell	166	246	266	270	277	266	282	266	281
3000 kg Brinell	166	250	246	255	268	261	274	263	266
Rockwell C (R_c)	N.M.	25.8	26.1	26.2	30.0	31.0	26.6	28.3	30.2
R_c in 500 kg Brinell	21.6	37.0	41.4	37.8	40.5	41.8	35.3	40.2	39.2
R_c in 1000 kg Brinell	22.7	39.8	42.5	41.6	43.1	44.3	41.2	42.6	41.2
R_c in 1500 kg Brinell	22.9	40.4	44.2	42.2	44.6	45.6	42.8	41.7	41.0
R_c in 2000 kg Brinell	22.4	42.1	43.9	42.5	45.0	44.8	42.2	41.6	40.4
R_c in 2500 kg Brinell	21.8	42.3	44.2	43.7	44.2	44.2	43.2	42.7	41.8
R_c in 3000 kg Brinell	23.0	42.8	43.1	42.1	44.6	45.6	42.2	42.2	39.8
R_c on broken tensile	N.M.	35.7	40.7	40.0	41.3	42.2	43.1	43.4	33.4
R_c in 3000 kg Brinell on broken tensile	N.M.	45.0	48.7	46.1	49.6	48.3	46.8	47.1	43.6
R_c in last of multiple overlapping 3000 kg Brinell dents	N.M.	52.7	49.2	50.6	46.2	47.3	52.1	47.6	42.5

N.M. = Not measured.

partly of the first layer of austenitic manganese weld deposit. The raised central portion (to be struck by the dropweight hammer) consisted entirely of austenitic manganese steel weld buildup. Two holes were drilled in the base of each test specimen to be able to rigidly bolt it to the anvil. This was done so that, after each removal of the specimen from the anvil for indentation depth measurement, the test specimen could be returned to the anvil and located where it would be struck again in precisely the same location.

The dropweight machine employed was designed for the ASTM E208 (Ref. 5) dropweight test. The standard anvil was replaced by a solid flat carbon steel anvil 3 ⅛ in. (80 mm) thick, 3 ⅜ in. (86 mm) wide and 9 ⅝ in. (245 mm) long. This anvil was rigidly bolted to the dropweight machine base, with drilled and tapped holes for anchoring the test specimen so that it would be struck by the hammer at the mid-length of the specimen with the cylindrical axis of the hammer perpendicular to the specimen length.

The hammer used in the dropweight test is the 1-in. (25.4-mm) radius half cylinder, hardened to 50 Rockwell C minimum as specified in the ASTM E208 standard (Ref. 5). The 130-lb (59-kg) hammer was dropped from a height of 10⅝ in. (271 mm), for a drop impact energy of 115 ft-lb (156 J). This energy was chosen because it was found to provide an appreciable, but not excessive, dent after one drop and was about the mid-range of the energies considered by Niconoff (Ref. 4). The depth of the indentation was determined after 1, 2, 3, 4, 10 and 20 drops using a micrometer to measure the distance from the bottom center of the dent to the bottom of the specimen. The sequence of testing was such that all specimens had received the same number of blows when a group of indentation depth measurements was made, but the order of testing for a given number of blows was randomized. Figure 4 shows a specimen after 20 drops. At 20 drops, the specimen began to bulge in the longitudinal direction, so the test was stopped. After all of

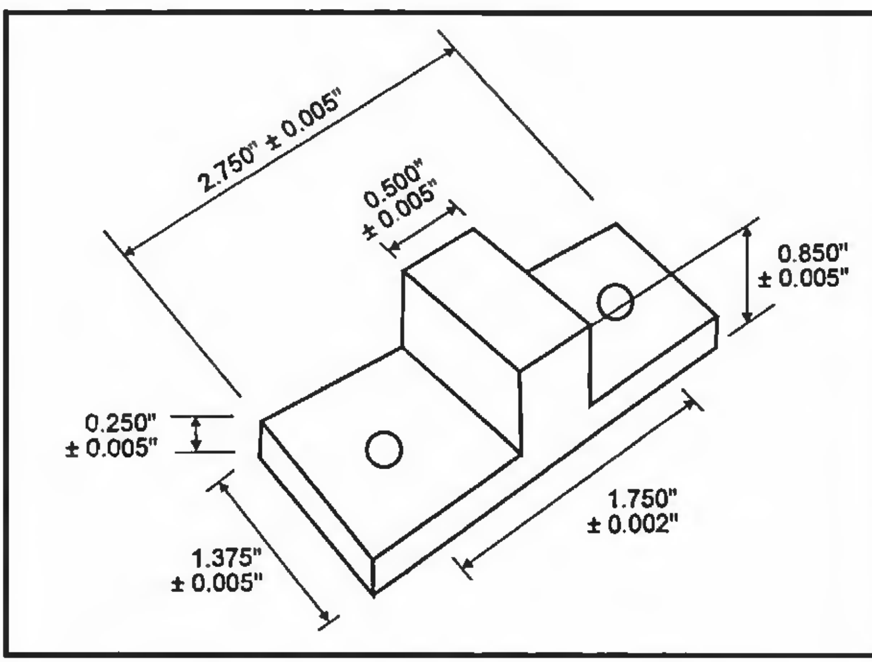

Fig. 3 — Schematic of dropweight test specimen machined from pyramidal deposit.

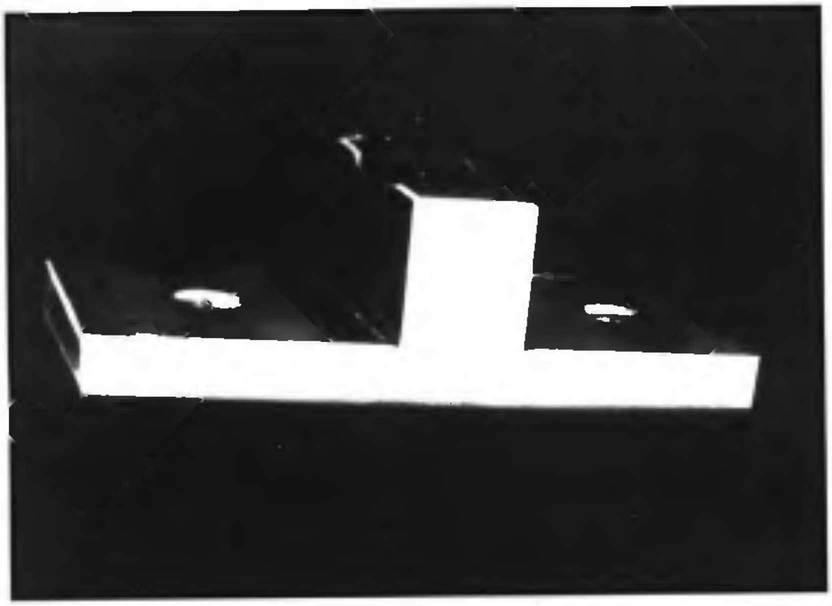

Fig. 4 — Dropweight test specimen after 20 impacts of 115 ft-lb (156 J) each.

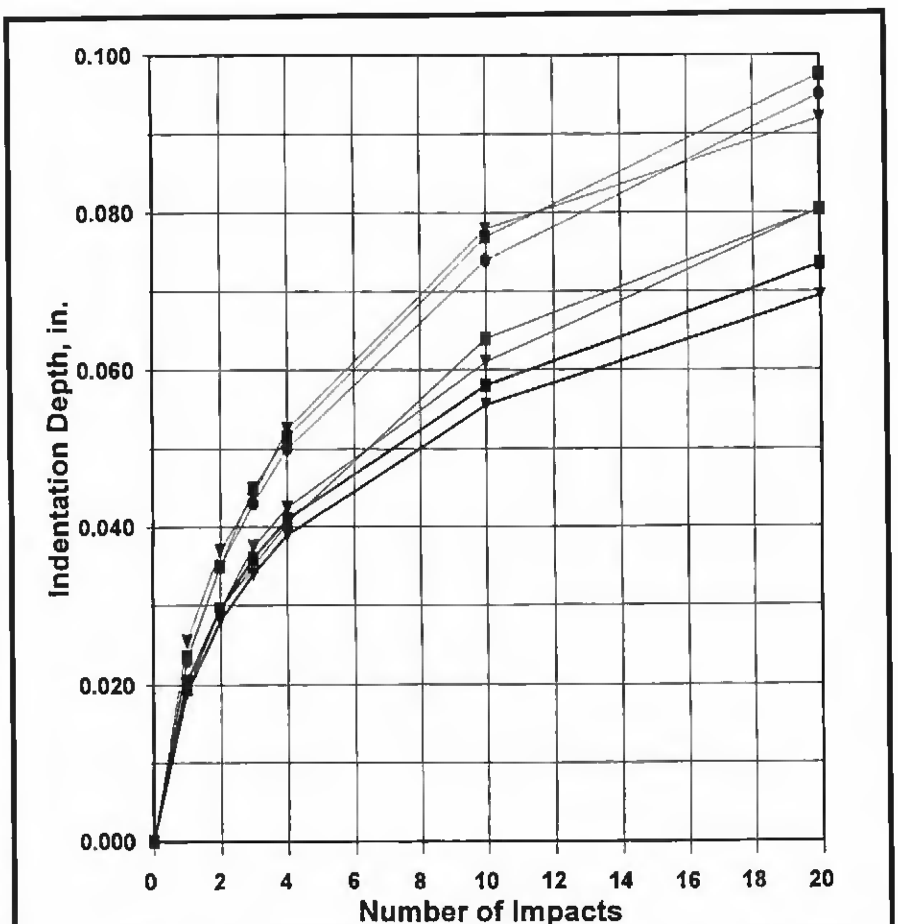

Fig. 5 — Dropweight indentation test results.

the dropweight tests were finished, the anvil was found to be only very superficially marked by the specimens, and the hammer was unmarked. So, essentially all of the dropweight energy went into deformation of the test specimens.

Experimental Results and Discussion

Deposit Compositions

The all-weld-metal chemical compositions for the wires are given in Table 2. Three examples are present from the ordinary austenitic manganese family (M14A, M14B and M14C). Two examples are present from the rich austenitic manganese family (M20A and M20B). And three examples are present from the austenitic manganese-chrome family (MC15A, MC15B and MC15C). It is apparent that none of the wires contains significant alloying with Mo or V. It is also apparent from Table 2 that there is considerable similarity among the deposit compositions within any one of the three alloy family groups.

The nitrogen analyses are noteworthy. Nitrogen is not a deliberate alloy addition to the wires; but, since the wires are deposited without shielding gas, nitrogen from the air can enter the arc and therefore the weld pool. Working with self-shielded flux cored stainless steel electrodes, which operate in a similar fashion to the austenitic manganese steel electrode compositions of the present study, Kotecki (Ref. 6) showed that deposit nitrogen increases with increasing voltage and decreases with either increasing current (wire feed speed) or increasing electrode extension. The electrodes in this study were all welded under the same conditions of voltage, wire feed speed and electrode extension (Table 1), but they have noticeably different slag systems. It is well known to those who formulate welding electrodes that, in general, slag systems high in fluorides such as fluorspar are more efficient than low fluoride slag systems at shielding the arc from nitrogen pickup in self-shielded FCAW. The highest deposit nitrogen was obtained with Electrode MC15C, the deposits of which consistently contained porosity and slag inclusions. The porosity with this electrode seems due to exceeding the nitrogen solubility limit for the alloy.

Tensile Tests

The all-weld-metal tensile test results are given at the top of Table 3. It can be seen that the three ordinary austenitic manganese deposits (coded M14 in the table) tend to have lower tensile strength and yield strength than the other two families of alloys, but there are large spreads in either tensile or yield strength within any of the three groups. It is noteworthy that one of the austenitic manganese-chrome deposits (MC15C) has markedly lower tensile elongation than the other two alloys in this family. This particular deposit contained numerous pores and slag inclusions, and it was found impossible to produce sound weld metal with it. None of the other deposits was found to contain such defects. These defects are likely to have caused the low tensile elongation of this material as well as the comparatively low tensile strength compared to yield strength. If that one elongation value is discounted, then there is a clear pattern of tensile elongation values among the three alloy families: all of the ordinary austenitic manganese deposits showed less than 20% elongation, the two rich austenitic manganese deposits showed percent elongation in the mid-twenties and the remaining two austenitic manganese-chrome deposits showed more than 30% elongation. The percent elongation values thus do appear to differentiate among the three families, but the meaning of this differentiation as it pertains to service on, for example, a rail frog, is unclear. In general, the deposits with higher percent elongation also exhibit higher ratios of tensile strength to yield strength, but the trend is not consistent — the M14B deposit, with only 19% elongation, has the highest ratio (1.497) of all, mainly because it has the lowest yield strength of all.

Brinell Hardness Tests

Turning to the Brinell hardness test results, Table 3 shows that all of the results, even those in the mild steel base metal, tended to be influenced by the load, reflecting, to some extent, work hardening. The 500-kg Brinell values for all of the austenitic manganese deposits were typically 50 points or more lower than the 2000-kg values. Oddly, however, all alloys except one (M14A) showed a slight decrease in Brinell hardness from the 2500-kg load to the 3000-kg load. Niconoff (Ref. 4) noted a similar "retrogression" in maximum surface hardness with increasing subsurface strain beyond a "point of satiation" in his austenitic manganese steels. All of the alloys showed similar increases in Brinell hardness with increasing load from 500 to 2500 kg, so this test is considered nondiscriminatory as it pertains to work hardening.

Rockwell C Tests

The Rockwell C hardness measurements without prior work hardening (Table 3) were 25 to 31 Rockwell C for all austenitic manganese alloys evaluated. Note that the electrode manufacturers' publications claim about 20 to 25 Rockwell C as-deposited for such alloys. However, the manufacturers' claims appear to be based upon measurements on the top surface of the last pass, not on the cross section of a multipass deposit as was used herein. Some cursory measurements on top surfaces of deposits confirmed the expected 20 to 25 Rockwell C hardness range there. The difference between top surface measurements and cross section measurements is probably due to some work hardening already taking place in the layers below the surface due to shrinkage strains from subsequent weld passes. For comparison, Niconoff (Ref. 4) found hardness values slightly below 10 Rockwell C for his annealed, strain-free austenitic manganese steels.

Table 4 — Meyer's Law Results, $P = Kd^n$

Composition		K = Penetration resistance	n = Strain hardening exponent
	A36 Base Metal	87.4	2.31
Ordinary austenitic manganese	M14A	118.2	2.42
	M14B	133.7	2.36
	M14C	92.3	2.68
Rich austenitic manganese	M20A	139.0	2.41
	M20B	121.0	2.46
Austenitic chrome-manganese	MC15A	132.6	2.42
	MC15B	129.7	2.39
	MC15C	146.9	2.34

Rockwell C Tests after Work Hardening

Rockwell C measurements in the reduced section of the broken tensile specimens (Table 3) were appreciably higher, mostly 40 Rockwell C. The two exceptions are M14A and MC15C, both whose tensile specimens fractured at the lowest percent elongation, 11% and 10%, respectively. These reflect lower work hardening before the Rockwell C test. In general, Table 3 shows increasing Rockwell C hardness after the tensile test with increasing percent elongation in the tensile test. Again, however, the relationship of this behavior to service performance is unclear.

The Rockwell C measurements in 500-kg Brinell dents in the austenitic manganese deposits all approached or exceeded 40 Rockwell C (Table 3). Further increase in Rockwell C values occurred with increasing Brinell load up to 2000 or 2500 kg, where all Rockwell C values were 40 to 46. As with the Brinell tests themselves, in several cases there was a drop in Rockwell C hardness in the 3000-kg Brinell dent as compared to Rockwell C hardness in the 2500-kg dent, again in agreement with the "retrogression" noted by Niconoff (Ref. 4). Here again, the tests proved to be nondiscriminatory among the alloy families since all compositions showed similar increases in Rockwell C hardness with increasing prior Brinell test load.

Testing in 3000-kg Brinell dents within the reduced section of the broken tensile test specimens produced Rockwell C values from 44 to 50 (Table 3), again with no clear discrimination among the alloys. In all cases, the Rockwell C value in the Brinell dent on the broken tensile specimen was higher than any of the Rockwell C values in Brinell dents on weld cross sections, *i.e.*, without additional work hardening from the tensile test.

Finally, after overlapping several 3000-kg Brinell dents in the weld cross sections to produce additional work hardening, Rockwell C measurement in the last dent of a cluster produced values as high as 52 Rockwell C (Table 3). In most, but not all, cases, this approach produced higher values than any of the other tests. It was interesting to note that values above 50 R_C could be obtained by this method. Niconoff (Ref. 4) found similar peak Rockwell C hardness values in his work hardened austenitic manganese steels. However, control of the degree of overlap among the multiple Brinell dents in the present study proved very difficult, so consistent results were not obtained. The method failed to provide any discrimination among the alloy types.

Meyer's Law

Another approach to discriminating among the austenitic manganese hardfacing alloy families was application of Meyer's Law (Ref. 7). Meyer's Law relates the applied load, P (kg), to the Brinell indentation diameter, d (mm), by

$$P = Kd^n \qquad (1)$$

where K is a material constant expressing resistance of the metal to penetration, and n is a material constant related to strain hardening of the metal. Since Brinell impressions were taken at various loads, it is easy to fit a regression equation of the Meyer's Law form to the data for each alloy and determine the best values of K and n. These can then be examined to see if there is any discrimination among the alloy families. This has been done in Table 4 where it is clear that there is no distinct grouping of alloy families according to the value of either K or n.

Dropweight Indentation Tests

A weld deposit from the one electrode that tended to produce deposits containing numerous pores and slag inclusions (Electrode MC15C) was not used in the dropweight indentation tests out of concern that the slag inclusions, noted previously, would damage the expensive ASTM E208 hammer. The other seven electrode deposits were subjected to this test.

The results of repeated dropweight indentation measurements are shown in Fig. 5. The indentation depth increases with an increasing number of blows from the dropweight hammer. Note that the indentation results in Fig. 5 cluster in three distinct groups, corresponding to the three alloy families. Beginning with the first hammer blow, the three ordinary austenitic manganese deposits exhibit greater indentation depth than do the other two families. This difference increases with increasing number of blows up to 20, at which point the test was stopped. This is clearly the least desirable performance of the three alloy families.

Although the remaining two austenitic manganese deposit families behave similarly as regards indentation resistance at up to four dropweight hammer blows, after 10 and 20 dropweight hammer blows, Fig. 5 shows that the rich austenitic manganese deposits separate from the austenitic manganese-chrome deposits, with the rich austenitic manganese deposits showing more indentation depth than the austenitic manganese-chrome deposits. This observation suggests that the austenitic manganese-chrome deposits will perform as well as or better than the rich austenitic manganese deposits in high impact service on a railroad frog.

It is beyond the scope of this project to try to determine the metallurgical reasons for the differences in resistance to deformation observed. One might speculate that transformation of austenite to martensite during deformation is involved. However, the richer alloys of the M20 and MC15 families would presumably be more stable metallurgically than the alloys of the M14 family; so, if anything, martensite transformation, if it occurs, would seem to work against improved indentation resistance. In the iron-manganese system, some martensite is ferromagnetic and some is not. With an instrument calibrated to the AWS A4.2 standard for ferrite measurement in austenitic stainless steel welds, magnetic response after the dropweight indentation tests equal to or less than 0.1 Ferrite Number was found in all of the deposits except M14B, the magnetic response of which was equal to 1.0 Ferrite Number. These are all very low levels of magnetic response, indicating little or no ferromagnetic martensite. Therefore, this is inconclusive.

Note that it is common experience in maintenance of railroad frogs that the rich austenitic manganese deposits outlast the ordinary austenitic manganese deposits, so most rail frogs today are rebuilt with the rich austenitic manganese deposits. The results of the dropweight indentation tests agree with that practice and experience. Railroad frog experience with the austenitic manganese-chrome family of deposits is limited. The authors are aware of one situation in which an austenitic manganese-chrome buildup on a railroad frog did not perform well, but that frog was welded with the MC15C electrode, which has been noted herein to tend to produce deposits with numerous pores and slag inclusions, resulting in low ductility deposits.

Note that the austenitic manganese-chrome deposit, containing typically about 15% chromium, is much more resistant to rusting than are the low chromium austenitic manganese deposits. As a result, these deposits tend to stand out visually on a rail line. This tends to create some resistance to their use on frogs. If a definitive service test shows that the austenitic manganese-chrome deposits, free of defects, can significantly outlast rich austenitic manganese deposits, then perhaps this resistance based upon visual appearance can be overcome. To the authors' knowledge, such a definitive test has not yet been made.

Conclusions

The objective of this experimental program was to find a test that could discriminate among the various families of austenitic manganese hardfacing deposits. Both as-welded hardness tests and hardness tests after various means of inducing work hardening produced nondiscriminatory results. Likewise, a Meyer's Law evaluation of strain hardening behavior proved inconclusive. Tensile and yield-strength measurements did not provide discrimination, but some discrimination appeared to be offered by the tensile elongation results — higher tensile elongation appears to correlate with better performance on railroad frogs. The most discriminating test, however, is the dropweight indentation test developed herein. This clearly separates austenitic manganese deposits into three groups. The dropweight indentation test shows significantly better indentation resistance of the rich austenitic manganese deposits as compared to the ordinary austenitic manganese deposits, which is in agreement with railroad frog performance experience. The austenitic manganese-chrome deposits performed still better in the dropweight indentation test, but correlating experience in railroad frog service is lacking.

The dropweight indentation test can thus be proposed as a screening test for austenitic manganese hardfacing deposits to evaluate resistance to heavy impact under controlled conditions.

References

1. Hadfield, R. A. 1884. U.S. Patent 303, 150.
2. Avery, H. S., and Chapin, H. J. 1954. Austenitic manganese steel welding electrodes. *Welding Journal* 33(5):459–479.
3. Fahrenwald, F. A. 1931. U.S. Patent 1, 815, 464.
4. Niconoff, D. 1941. Quantitative measurement of strain hardness in austenitic manganese steel. *Transactions of the A.S.M.* 29: 519–540.
5. ASTM E208-91. Standard test method for conducting drop-weight test to determine nil ductility transition temperature of ferritic steels. 1993. *Annual Book of ASTM Standards*, Vol. 03.01.
6. Kotecki, D. J. 1978. Welding parameter effects on open-arc stainless steel weld metal ferrite. *Welding Journal* 57(4):109-s to 117-s.
7. Dieter, G. E. 1976. *Mechanical Metallurgy*. Tokyo, Japan, McGraw-Hill, Kogakusha, Ltd., pp. 391–392.